Effects of Hind Limb Unloading and Spaceflight on Structural Properties of the Proximal Tibia

By
Taylor Comte

Senior Honors Thesis
Biomedical Engineering
University of North Carolina at Chapel Hill

April 6, 2015

Approved:

_____

Ted Bateman, Thesis Advisor

Anthony Lau, Reader

Shawn Gomez, Reader

Abstract

Unloading during spaceflight alters the microstructure of bone resulting in a significant reduction in bone health. Hind Limb Unloading (HLU) in mice is used to study the musculoskeletal changes caused by spaceflight. This study investigates the effects of HLU on bone stiffness and structural efficiency using Finite Element Analysis (FEA) on the proximal tibia of mice from a HLU study mimicking space shuttle mission STS-135 (13-days of spaceflight). Structural bone health was compared between HLU and spaceflight in terms of bone stiffness and structural efficiency as well as their response to Sclerostin antibody (Scl-Ab). HLU and spaceflight had the same effect on BV (-17%); however, spaceflight caused a greater decrease in stiffness (-34%) compared to HLU (-22%). Scl-Ab prevented the loss of BV and stiffness in the HLU and spaceflight groups. The spaceflight model showed a greater decrease in structural efficiency (-22%) between the flight vehicle and ground control groups compared to HLU (-5%).The difference in structural efficiency from unloading can be attributed to the incomplete unloading in HLU. Future studies should investigate the mechanisms resulting in the changes in structural efficiency to further characterize differences in the HLU model and microgravity in spaceflight.

Introduction

Spaceflight and bedrest cause a -.35% reduction in total Bone Mineral Density (BMD) per month, reducing the bone health of astronauts and patients on bedrest significantly (LeBlanc et al., 1996). Investigating the structural changes caused by microgravity conditions can lead to improved therapies for an expansive population affected by bone disease and bed rest. There are over 70 million people worldwide at risk for fractures which have been shown to significantly increase morbidity (Boyle, Simonet, & Lacey, 2003). Mortality rate increases from 3% to 14.8% after operation for proximal femoral fractures for people over 50 years old (Sexson & Lehner, 1987) . The clinical significance is most important for patients with osteoporosis, especially for women who are at higher risk due to the 7.2% incidence of new vertebral fractures within 3 years post menopause (Bone et al., 2013).

Sending mice to space allows rapid testing of bone loss countermeasures, because of the rapid turnover rate of bone in microgravity environments. Ground models approximating the effects of unloading seen in mice sent to space allow less expensive means of testing drugs and studying bone remodeling (Morey-Holton & Globus, 2002). Furthermore, spaceflight experiments provide critical information about the health of astronauts (Morey-Holton & Globus, 2002). The goal of this study was to investigate the structural changes of tibia bones due to Hind Limb Unloading (HLU) in mice, including differences in trabecular and cortical compartments.

To accomplish the objective of this study stiffness normalized by bone volume was determined with Finite Element (FE) modeling from micro Computed Tomography (microCT) scans. The contribution of cortical and trabecular components to bone volume, effective stiffness, and structural efficiency of the whole bone was investigated to provide more detailed

information. Additionally, the bone loss countermeasure, Sclerostin Antibody (Scl-Ab), was administered to sub groups of the HLU and spaceflight study groups to analyze differences in effectiveness of the drug in the 2 unloading conditions.

Background

Bone is comprised of mineralized and nonmineralized (osteoid) tissue. In long bones such as the femur and tibia, cortical bone is the outer region that supports most of the uniaxial load applied to the body. The other major component is trabecular bone, the inner region of long bones consisting of trabeculae struts of about 167μm thick that support smaller loads but in many directions (Ding & Hvid, 2000). Bone marrow is located in the center along the length of long bones. Cortical bone is dense and organized in a haversian system which consists of concentric layers (lamellae) of bone tissue around a central haversian canal (osteon) where blood vessels are located. There are 3 bone cells that control bone remodeling: osteoblasts that form new bone, osteoclasts that remove bone, and osteocytes that function as mechanotransducers. Bone cells communicate by signaling molecules or direct contact through small canals called canaliculi. (Boskey & Robey, 2013)

Bone remodeling occurs throughout life at a rate of 4 to 10% per year and is dependent on many environmental factors including diet, estrogen levels, and exercise (Franz-Odendaal, Hall, & Witten, 2006). The balance of osteocytes and osteoblasts controls bone health. This balance is achieved through signaling molecules and cell-cell interactions. For example, the formation of bone resorptive cells, osteoclasts, require cytokines especially Receptor Activator of Nuclear Factor Kappa-B Ligand (RANKL) which prime precursor cells; however other cytokines such as osteoprotegerin (OPG) inhibit RANKL. When activated, osteoclasts isolate their acidic environment to the surface of bone which exposes the organic matrix, mainly type I collagen that is degraded by the lysosomal enzyme cathepsin K. Integrins are essential for attaching the osteoclasts to the bone matrix. Also important in the bone resorption process are the ruffled zone which is formed when osteoclasts attach to the bone surface, and the sealing zone which restrains the acidic environment to the surface of the bone matrix. Discoveries in bone resorption have mainly stemmed from biochemical and molecular experiments, and experiments with mice lacking specific genes. (Ross, 2013)

Cytokines are also important for osteoblast differentiation from mesenchymal stem cells. Hedgehogs, Bone Morphogenetic Proteins, Transforming Growth Factors, Parathyroid Hormones, and Wingless-related Integration sites (Wnt) are all involved in initiating the signal transduction cascades necessary for osteoblast differentiation (de Gorter & ten Dijke, 2013). When the bone forming phase is complete, some osteoblasts become lining cells (deactivated) and some undergo apoptosis (Franz-Odendaal et al., 2006). Other osteoblasts slow down production of bone matrix and become buried by matrix from other osteoblasts, thereby becoming osteocytes (Franz-Odendaal et al., 2006). Osteocytes are the most abundant bone cell, making up 90-95% of all bone cells (Franz-Odendaal et al., 2006). They are distributed throughout mineralized matrix, and have long dendritic processes that extend through the canaliculi from the bone marrow to the bone surface (Bonewald, 2013).

Sclerostin Antibody

Sclerostin is a protein encoded by the SOST gene that regulates osteoblast activity by interfering with its development through the Wnt pathway and triggering apoptosis. In diseases such as Sclerosteosis and Van Buchem, the SOST gene has mutations in the coding region or a regulatory region downstream which prevents sclerostin production or down regulates it respectively. These conditions result in abnormally high levels of bone growth. Sclerostin Antibody (Scl-Ab) works in a similar manner, preventing the function of sclerostin so that more bone growth occurs. (Yavropoulou, Xygonakis, Lolou, Karadimou, & Yovos, 2014)

Mouse Model

C57Bl/6 mice have been extensively used to study bone loss. Their skeletal growth is similar to human bone growth. Several studies have shown that peak volumetric Bone Mineral Density (vBMD) is achieved between 3-6 months of age; however, ash fraction, representing the tissue level density, does not change significantly from 4 to 24 weeks (Somerville, Aspden, Armour, Armour, & Reid, 2004). This indicates that material density of bone remains constant, while mineral content increases (Somerville et al., 2004). These results were also supported by Silva et al., whose work determined that peak bone strength of C57Bl/6 female mice is not reached before 20 weeks of age, and that densitometric properties remained constant from 4-24 weeks (Brodt, Ellis, & Silva, 1999). Bone loss with aging in C57Bl/6 mice has also been documented to be similar to human bone loss (Halloran et al., 2002). Humans reach peak BMD between 10-19 years of age; however Bone Mineral Content (BMC) continues to increase to 30-35 years of age (Halloran et al., 2002). This trend in bone growth occurs because radial growth of bone and increased mineralization occurs after peak BMD is reached (Halloran et al., 2002). After bone growth, BMD and BMC decrease with age (Halloran et al., 2002). The male C57Bl/6J mice used in this study reached peak bone mass at 12-13 months, about half of their life span, similar to humans (Halloran et al., 2002).

The mouse skeletal system is similar to human bone; however there are some important differences. C57Bl/6 mice lack the cortical organization present in the haversian system of human cortical bone (Jilka, 2013). Thus, remodeling of cortical bone in mice and humans occurs in different manners. Bone turnover in mice is about 0.7% per day measured in the distal femur and each remodeling episode takes 2 weeks to complete (Jilka, 2013). In contrast, human bone at the iliac crest turns over at about 0.1% per day and each event takes about 6-9 months to complete (Jilka, 2013). The quick turnover rate of mouse bone makes them useful for modeling bone loss in humans. Mouse trabeculae are between 20-50μm thick, whereas human trabeculae are about 167μm thick, which is important when considering imaging techniques to quantify changes in trabecular microstructure (Christiansen, 2013).

Imaging

Dual-energy X-ray Absorptiometry (DXA) is a type of imaging used to assess bone health by quantifying BMD. However, BMD only moderately correlates with bone strength which is the best predictor of fracture risk. Improvements in imaging techniques have allowed

for the analysis of microcracks in cortical bone and trabecular bone architecture, contributors to overall bone strength. With current improvements in imaging techniques, it is expected that knowledge of microarchitecture of bone can eventually be used in the clinical setting to assess bone strength. Peripheral Quantitative CT (pQCT) can be used to analyze trabecular architecture in large animals and cadaver bones; however, the resolution (70μm) is too low for analysis of trabeculae in rodent models. Radiation dose from QCT scans prevent its use to analyze the hip in the clinical setting. Furthermore, partial volume averaging needs to be considered with low resolution imaging, especially if trabecular bone is being analyzed (167μm thick trabeculae). MicroCT can obtain resolutions up to 5um, allowing analysis of rodent trabecular architecture. With the discovery of synchrotron radiation (resolution <1μm), and forms of MicroCT scanners that can be used in vivo, clinical assessment of bone health should improve. (Christiansen, 2013)

Spaceflight Model

Lang et al. has investigated bone loss in astronauts from long duration spaceflight in terms of BMD and bone geometry using QCT and DXA, and Keyak et al. has investigated bone strength of astronauts using FE modeling. Lang et al. used volumetric QCT to analyze integral, cortical and trabecular vBMD in the hip and spine after long duration missions (4-6 months). They found a decrease in vBMD at 1.2-1.5%/month in the hip, with .4-.5%/month from cortical, and 2.2-2.7%/month from trabecular bone. (T. Lang et al., 2004)

Lang, et al. also showed that reloading after spaceflight allows bone mass to recover but not vBMD. The loss of bone mass occurred by thinning of the cortex from the inner margin without compensatory periosteal apposition as seen in the aging process. They also found that new bone was less mineralized or more porous than what was previously lost, causing the slow recovery of vBMD. (T. F. Lang, Leblanc, Evans, & Lu, 2006)

In a Flight Analog Study, human subjects participated in a head-down bed rest study showing similar BMD reduction to spaceflight in hip, pelvis, and heel (1%/month) (Spector, Smith, & Sibonga, 2009). These studies indicate the importance of developing countermeasures for bone loss from unloading conditions such as microgravity and bed rest.

Hind Limb Unloading Model

The HLU model established in 1979 by NASA Ames Research Center has been accepted and widely used to study the musculoskeletal changes caused by spaceflight (Morey-Holton & Globus, 2002). In this model mice experience: differential muscle atrophy, cephalad fluid shift, freedom to use forelimbs normally, ability to recover from unloading, and normal weight gain in young mice and normal weight loss in adult mice throughout the experiment (Morey-Holton & Globus, 2002). This study investigates bone changes in HLU, because research has shown similar declines in mineral density as seen in mice flown to space (Morey-Holton & Globus, 2002). Although current evidence supports the model's approximation of BMD loss in spaceflight, no studies have investigated the stiffness of the bone using Finite Element Analysis (FEA).

Finite Element Analysis

FEA is used to simulate mechanical testing on bone to estimate bone strength without destroying the bone sample. With improved imaging and computational techniques, measures of bone strength can eventually be used for clinical diagnosis of osteoporosis, since BMD only moderately predicts bone strength. Keyak et al. showed that CT based nonlinear FE modeling of the proximal femoral strength estimated fracture risk better than areal BMD. (Keyak et al., 2013)

In mechanical testing, failure load is the most important factor that determines fracture risk. It is a measure based not only on the amount of bone mass present, but also on the spatial distribution of trabeculae. Bone failure load determines the point at which the bone fails mechanically. In experimental compression tests, it is the load peak after which a decrease in load of at least 5% is observed on a force-displacement curve. (W Pistoia et al., 2004; Walter Pistoia et al., 2002) Pistoia et al. determined that the optimal parameters for μFE simulation prediction of failure load is obtained by setting a critical limit for which the bone tissue begins to fail. Literature has used 7000 microstrain as this critical limit based on strain energy density and young's modulus of bone. The failure load in FE simulations is determined by the load at which more than 2% of the bone is strained beyond the tissue yield strain.(Walter Pistoia et al., 2002)

Pistoia et al. used an isotropic and linear-elastic model with E=10GPa and v=0.3. However, bone is anisotropic, responding differently to loads applied in different directions. Additionally, cortical bone is stronger in compression than tension, making it a nonlinear material (Niebur, Feldstein, Yuen, Chen, & Keaveny, 2000). The assumptions of the model allow reasonable CPU time and memory allocation, although a nonlinear anisotropic model would predict failure load more accurately (Niebur et al., 2000).

Keyak et al. used a nonlinear FEM with isotropic material properties to estimate proximal femoral strength. Ash density computed from the CT scanner was used to set a unique elastic modulus and material strength to each pixel using correlations previously determined for trabecular and cortical bone. After material failure, plastic flow was modeled with post failure properties based on ash density and previously reported correlations originally obtained for trabecular bone. They found the fall configuration for loading was better approximated by nonlinear models. (Keyak, 2001)

Pistoia et al. used μFE based on images of 3D-pQCT images to show that bone mass measurements of the radius were poor predictors of failure load. The best predictor was BMC (R^2=0.48). However, the μFE simulation estimated failure load with R^2=0.75. Several structural parameters including a combination of Trabecular Number (Tb.N), Trabecular Threshold (Tb Th), Bone Volume Fracture (BT/TV), and Cortical Thickness (Cth) were also tested for ability to predict failure load (R^2=0.57). (Walter Pistoia et al., 2002)

Pistoia et al. used the same procedure to test a 1cm cross section of the radius. The results indicated that a μFE simulation of a small cross section of the radius is a better predictor for failure load compared to bone mass measurements and structural parameters; however, there is a reduction in coefficient of determination (R^2=0.66) compared to simulations based on the whole radius. Measurements based on a small portion of bone will be important for moving from bench

to bedside, since more imaging data will require more time and CPU power. (W Pistoia et al., 2004)

Literature has used QCT, pQCT, and DXA with a range of resolutions to model bone and produce FE models. Pistoia used pQCT to model human radius bones and to estimate failure load. Keyak used QCT and nonlinear FEMs to estimate human femur and vertebrae failure loads. This study uses microCT scans of mouse tibia bones with resolution of 10μm to obtain accurate representation of both cortical and trabecular bone microstructure. Since failure load assumes material properties of bone such as yield stress and point of fracture are known, this study uses stiffness as the main structural parameter. Stiffness is similar to failure load, except the material isn't deformed past the tissue yield strain, which requires well known material properties of cortical and trabecular bone and a nonlinear model [kayak 2001]. Stiffness will be used to demonstrate the force (N) required to compress the structure by .5%.

Materials and Methods

Study Design

The HLU experiment was designed and performed by Mary Bouxein at Harvard University. The protocol was made to mimic the STS-135 space shuttle spaceflight experiment where mice were exposed to microgravity conditions for 13-days. Mice on STS-135 were housed in the animal enclosure model developed by NASA to provide mice living space, food, water, ventilation, and lighting (Wigley, 2012). Table 1 provides a brief description of the two studies. A total of 60 female C57BI/6C mice 9 weeks of age at the start of the experiment were included in this study. The mice were acclimated to wire floors and fed with Nutrient-upgraded Rodent Food Bars according to NASA Ames protocol for 2 weeks prior to the experiment (Wigley, 2012). Bone mineral density was measured 3 days before the start of the experiment using DXA under inhaled isoflurane anesthesia for about 8 minutes. One day prior to the start of the experiment, all mice received 2 subcutaneous injections to the back of either drug or vehicle and celcein bone label to detect developing bone. To begin the experiment HLU mice were put into tail suspension under inhaled isoflurane anesthesia for about 5 minutes, while control mice were exposed to a similar duration of anesthesia.

29 mice were in HLU for 13 days in which 15 received Sclerostin Antibody (Scl-Ab) as a countermeasure for bone loss. The control group consisted of 29 mice in which 15 received Scl-Ab countermeasure. These groups were not subjected to HLU but maintained all other aspects of the experimental group. To simulate reloading from spaceflight, the HLU mice were removed from their harness 3 hours prior to the beginning of dissection. All mice were completely dissected within 30 minutes of death. A 1.0mm thick cross section of the proximal tibia just inferior to the growth plate was dissected for microCT scanning and FE modeling.

Table 1: HLU and Spaceflight Experiment Design

Group	**Size**	**Treatment**	**Description**
HLU Ground Control	n=15	Placebo	Housed in Cages with No Tail Suspension
	n=15	100mg/kg Scl-Ab	
HLU	n=15	Placebo	Housed in Cages with Tail Suspension
	n=15	100mg/kg Scl-Ab	
Ground	n=15	Placebo	Housed in AEM at Kennedy Space Center
	n=15	100mg/kg Scl-Ab	
Spaceflight	n=15	Placebo	Housed in AEM on Space Shuttle Atlantis: STS-135
	n=15	100mg/kg Scl-Ab	

FEA Modeling and Simulation Procedure

The proximal tibia was scanned with a Scanco microCT scanner at 10μm resolution. A threshold of 375mgHA/cm^3(205 per mille) was chosen to include trabecular bone.These were used to generate subject specific FE models of each tibia bone. The microCT images were imported into ABAQUS CAE 6.9 for FE modeling and simulation. **Figure 1** shows the models produced by the scans. Bone material properties were assumed to be homogenous (E=10 GPa, ν=0.3). Bone stiffness was calculated as the resultant force (N) from the applied displacement (mm). Structural efficiency, an indicator of how structurally efficient the bone is arranged, was calculated as the stiffness per bone volume.

The superior and inferior surfaces of the tibia were initially fixed. A load was applied to displace the superior surface by .5%. The force at each node required to displace the surface .005mm was summed so that stiffness could be taken as the force per mm of displacement. The volume was calculated as the number of cuboidal elements in the mesh multiplied by the volume of each element ($9.99\times 10^{-7} mm^3$). The structural efficiency of the bone was defined as the stiffness per total bone volume. These large FE problems, with on average 1 million elements, were solved using 3 CPUs and 38Gb of memory for each model, requiring approximately 40 min. per model to complete the output database file.

A separate mesh was generated using the proprietary Scanco software for cortical bone so that any differences in bone volume, stiffness, or structural efficiency between cortical and trabecular bone could be determined. **Figure 2** shows a model before and after separation of cortical bone from whole bone. The same simulation was used for these meshes, and trabecular bone volume and stiffness was calculated as the difference between the whole and cortical bone values. Structural efficiency of trabecular bone was calculated from these results.

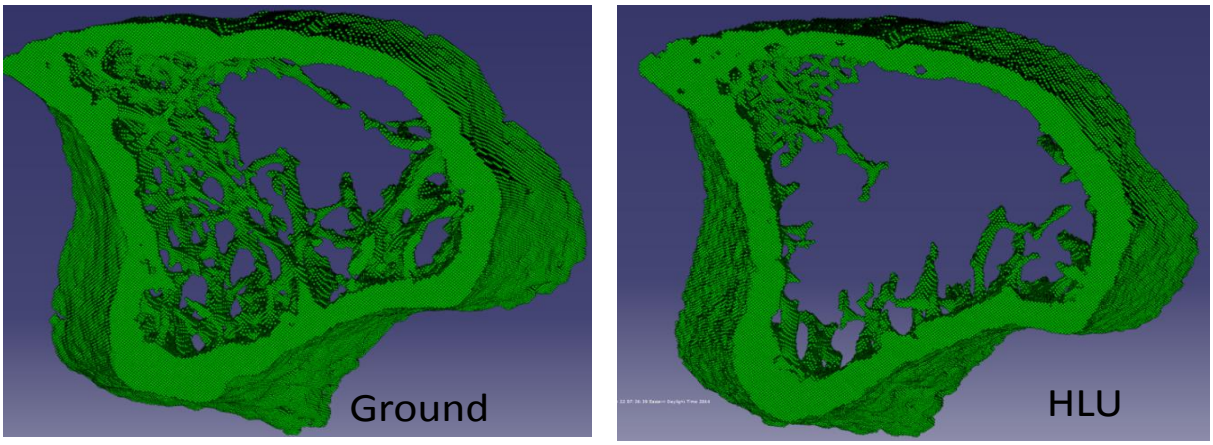

Figure 1: The figure above shows the finite element models produced from the microCT scans of mouse proximal tibia bones from a ground control group (Left) and a HLU group (Right).

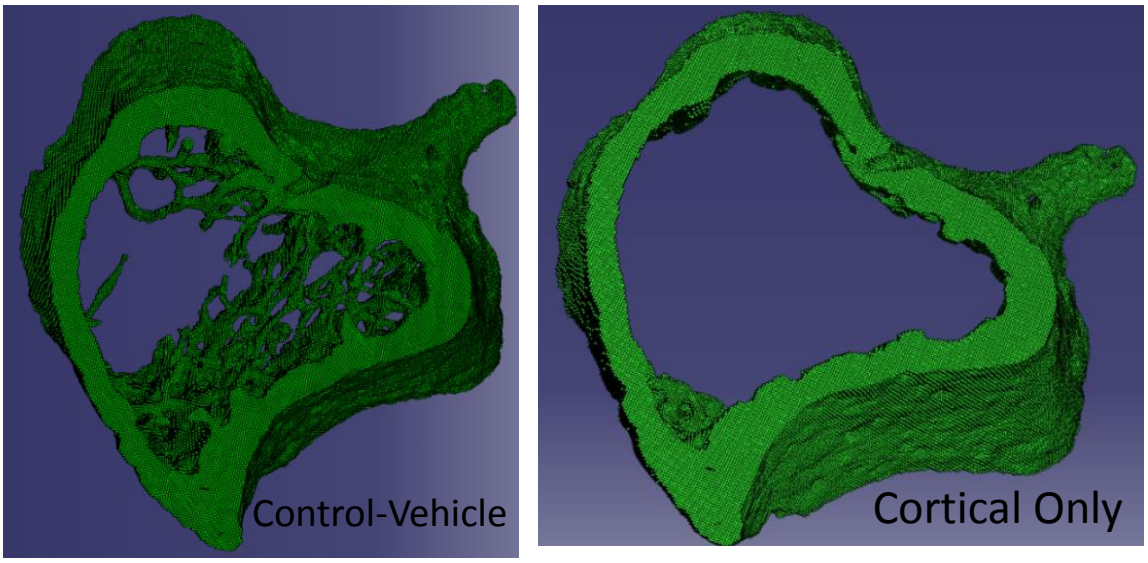

Figure 2: The figure above shows a ground control model of whole bone (Left) and the subsequent model after extraction of the trabecular bone (Right).

Statistical Analysis

Results are presented as mean ± SEM. Two way Analysis of Variance (ANOVA) analysis was used to establish the statistical significance of the data with $p \leq .05$ being significant, signified in graphs with a * symbol. The Tukey Test was used to determine significant differences between groups only when the ANOVA resulted in $p \leq .05$. Bone volume, stiffness, and structural efficiency were analyzed using this method. Qualitative comparisons were made between HLU and spaceflight groups.

Results

Figure 3 (a,b), shows the effect of HLU on bone volume and stiffness, as well as the effectiveness of Scl-Ab in the ground groups and HLU groups. HLU caused significant reductions in bone volume and stiffness, and Scl-Ab caused significant increases in bone volume

and stiffness with $p<0.05$. HLU resulted in a greater decrease in stiffness (-22%) compared to bone volume (-17%). Scl-Ab was more effective in the HLU condition compare to the ground controls with 48% and 37% increase in bone volume respectively. Scl-Ab caused a greater increase in stiffness (48%) compared to bone volume (37%) in the ground controls as well as the HLU groups (61% and 48% for stiffness and bone volume respectively). Overall, Scl-Ab recovered the loss in bone volume and stiffness from HLU.

Shown in **Figure 3 (c,d)** are the counterparts of a and b for spaceflight. Spaceflight stiffness did not pass the normality test, and should be taken into consideration when analyzing results. Spaceflight also caused a significant -17% reduction in bone volume; however, the decrease in stiffness (-34%) was greater in spaceflight compared to HLU (-22%). The increase in bone volume in HLU from Scl-Ab (48%) was greater than the increase in spaceflight from Scl-Ab (39%), but the ground controls for spaceflight showed a greater increase in bone volume from Scl-Ab (42%) compared to HLU (37%). The difference in the effects of Scl-Ab were greater in stiffness with the HLU experiment's ground control experiencing a 48% increase in stiffness compared to a 60% in the ground control groups from the spaceflight study. However, Scl-Ab still caused a similar increase in stiffness for both HLU (61%) and spaceflight (62%) groups.

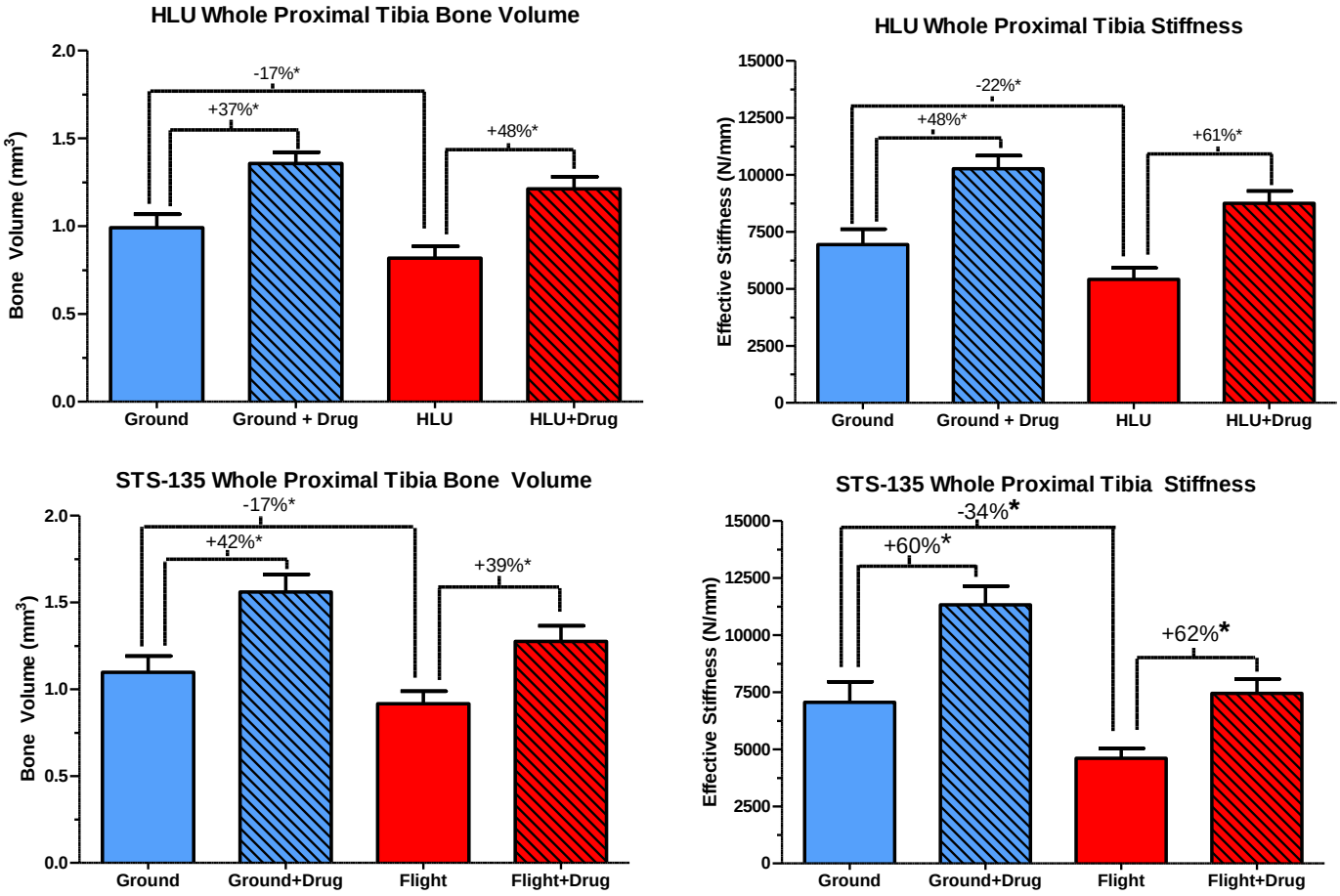

Figure 3 (a,b,c,d left to right, top to bottom): Shown above are the BV and stiffness results for whole bone. The percent change is noted along with the significance *($p<0.05$). BV and stiffness results for HLU are shown in a and b respectively. BV and stiffness results for spaceflight are shown in c and d respectively.

Figure 4 (a,b) shows the cortical compartment bone volume and stiffness results from the HLU groups. HLU caused a significant decrease in cortical bone volume (-10%) and stiffness (-15%) with $p<0.05$. The increase in bone volume and stiffness from Scl-Ab was significant ($p<0.05$) in each of the ground groups, and recovered what was lost from HLU. Similar to whole bone, cortical bone stiffness was affected more by Scl-Ab compared to bone volume.

Shown in **Figure 4 (c,d)** are the counterparts to a and b for spaceflight. Spaceflight cortical efficiency failed normality and equal variance test, and should be taken into account when analyzing results. There was a slightly greater decrease in bone volume from spaceflight (-14%) compared to HLU (-10%). A larger difference between HLU and spaceflight occurred for stiffness with a 15% decrease from HLU and a 32% decrease from spaceflight. Similar to whole bone, cortical bone had greater increases in bone volume and stiffness from Scl-Ab while in the HLU condition (35%, 52%) compared to the ground controls (24%, 34%). However, in the spaceflight groups, Scl-Ab was more or equally effective in the ground controls (33%, 48%) compared to the spaceflight groups (31%, 48%) for bone volume and stiffness respectively. In all cases, Scl-Ab recovered cortical bone volume and stiffness lost by unloading.

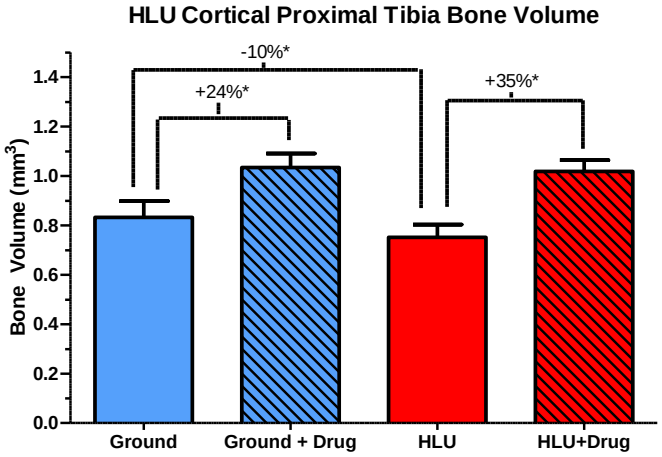

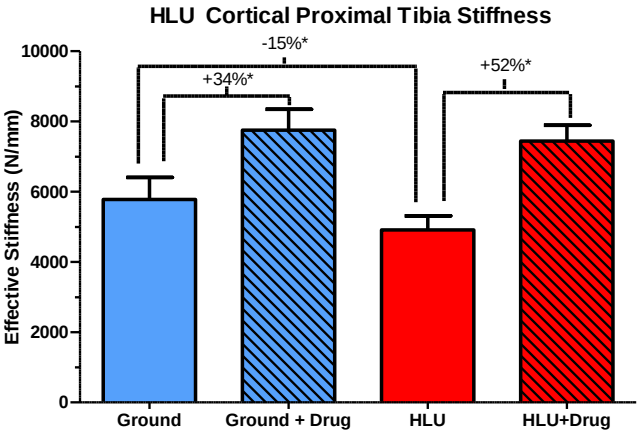

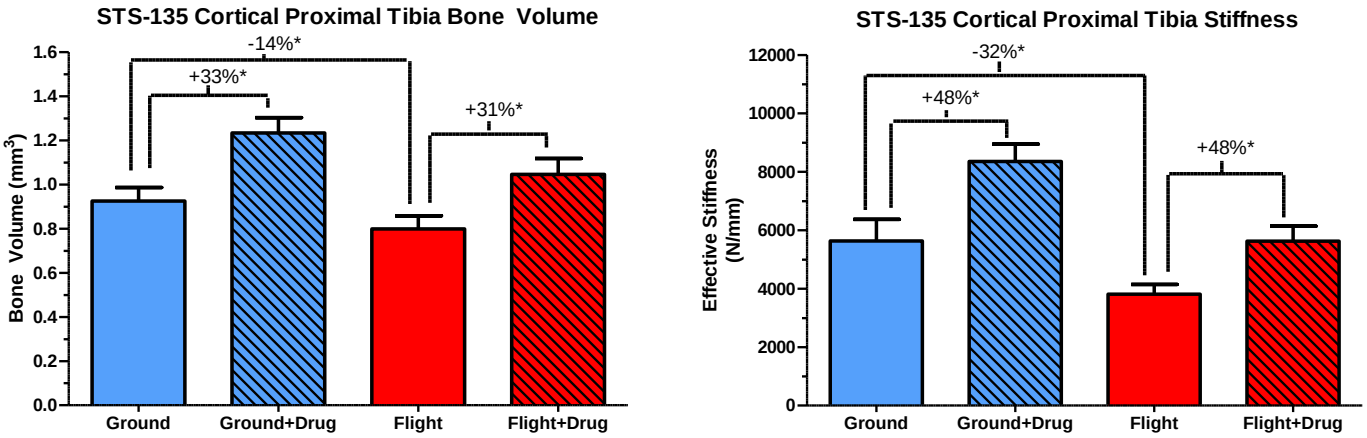

Figure 4 (a,b,c,d left to right and top to bottom): Shown above are the BV and stiffness results for cortical bone. The percent change is noted along with the significance *($p<0.05$). BV and stiffness results for HLU are shown in a and b respectively. BV and stiffness results for spaceflight are shown in c and d respectively.

Figure 5 (a,b) shows the effect of HLU on trabecular bone volume and stiffness. The trabecular compartment failed to pass the equal variance test, because trabecular bone is sparser than cortical bone, and the study was limited to 15 mice per group; however this failure should be taken into account when analyzing resutls. HLU caused a significant decrease in bone volume (-58%) and stiffness (-56%). In contrast to whole and cortical bone, trabecular bone volume decreased slightly more than stiffness. Scl-Ab caused significant increases in bone volume and stiffness in the ground and HLU groups. Also similar to whole and cortical bone results, Scl-Ab had a greater effect on trabecular bone volume and stiffness in the HLU groups (194%, 156%) compared to ground controls (104%, 117%).

Shown in **Figure 5 (c,d)** are the counterparts to a,b for spaceflight. Unlike the effect in HLU, spaceflight caused a greater decrease in trabecular bone stiffness (-45%) compared to trabecular bone volume (-32%). Similar to all other results, Scl-Ab had a greater effect on bone volume and stiffness in the unloading condition (+95%, +131%) compared to the ground controls (+88%, +108%). In contrast to cortical bone results, trabecular bone volume decreased more from HLU (-58%) compared to spaceflight (-32%). Trabecular stiffness also decreased more from HLU (56%) compared to spaceflight (-45%). Scl-Ab caused greater increases in bone volume and stiffness in the HLU condition compared to spaceflight; however, the HLU ground controls also had greater increases in bone volume and stiffness from Scl-Ab compared to the spaceflight ground controls.

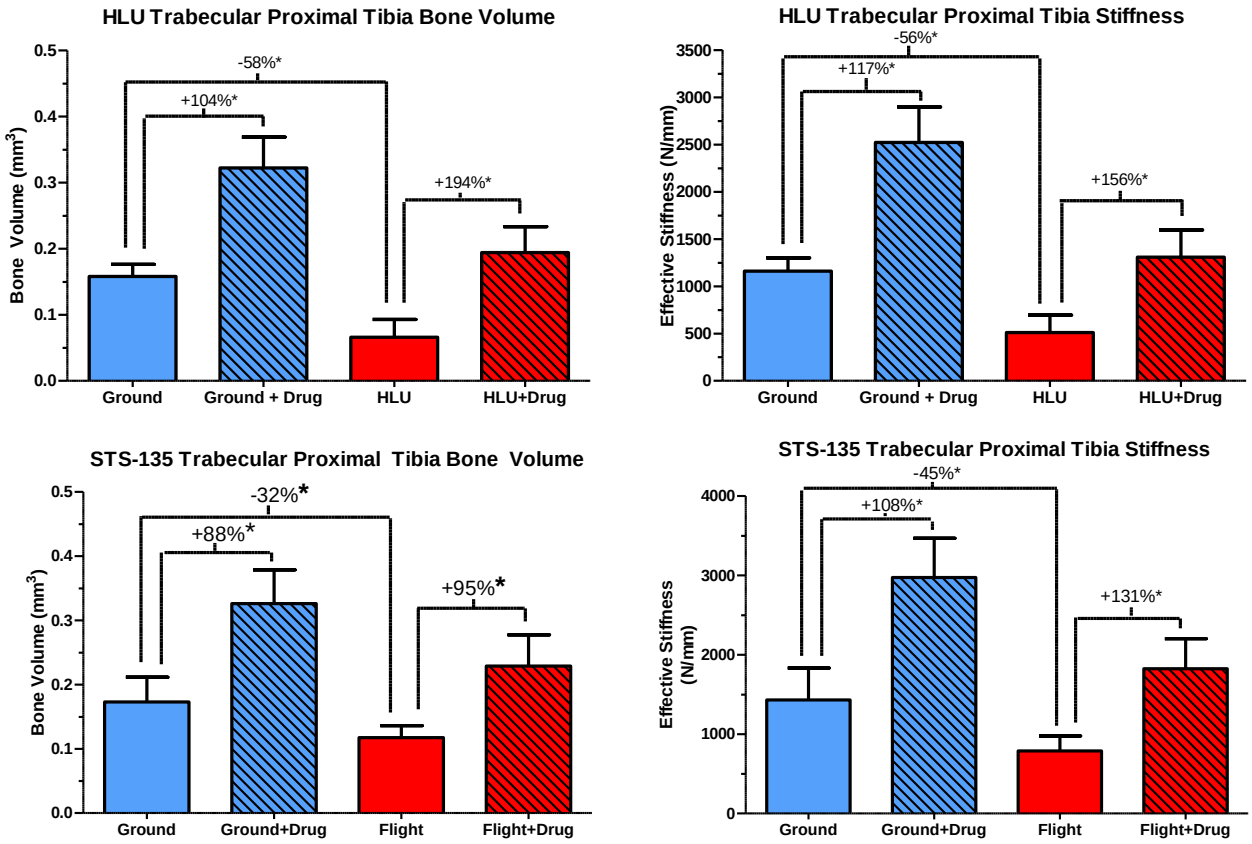

Figure 5 (a,b,c,d): Shown above are the BV and stiffness results for trabecular bone. The percent change is noted along with the significance *($p<0.05$). BV and stiffness results for HLU are shown in a and b respectively. BV and stiffness results for spaceflight are shown in c and d respectively.

Figure 6 (a,b) shows the effect of HLU and spaceflight on structural efficiency of whole bone. Spaceflight caused a greater decrease (22%) in structural efficiency compared to HLU (5%). Scl-Ab caused a greater increase in structural efficiency in the spaceflight study compared to HLU in both the ground groups (13%,8%) and unloaded groups (16%,9%). Cortical bone structural efficiency followed a similar trend to whole bone results. Spaceflight also caused a similar effect on trabecular bone structural efficiency; however, HLU caused a different response in trabecular bone structural efficiency. There was not a significant difference between the HLU ground control group and the HLU ground group with Scl-Ab. Additionally, HLU caused a 8% increase in trabecular structural efficiency. Furthermore, the HLU group with Scl-Ab had a 16% reduction in structural efficiency compared to the HLU placebo group.

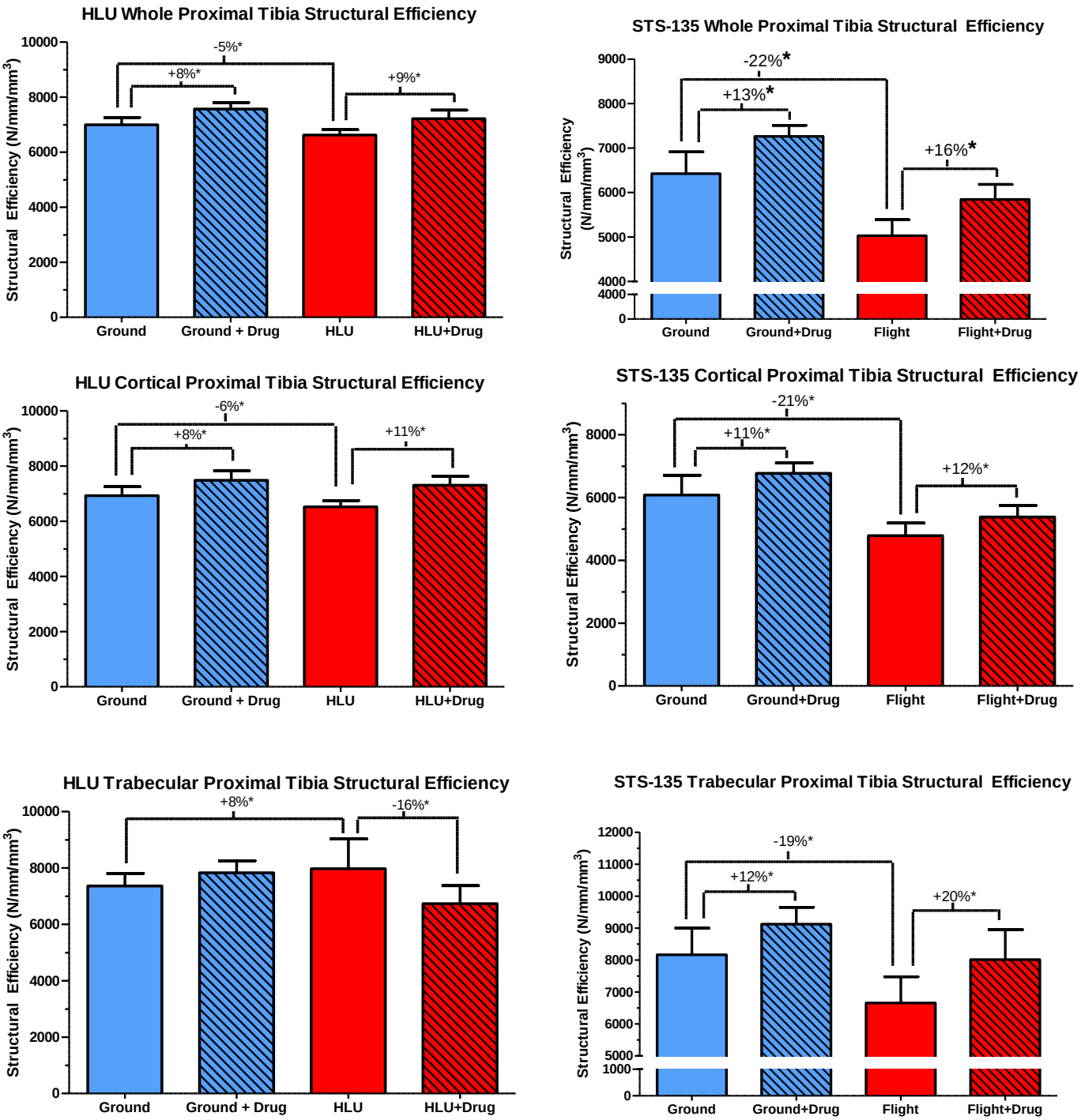

Figure 6 (a,b,c,d,e,f): Shown above are the efficiency results for whole (a,b), cortical (c,d), and trabecular bone (e,f) with HLU in the left column and spaceflight in the right column. The percent change is noted along with the significance *($p<0.05$). BV results for HLU and spaceflight are shown in a and b respectively. Stiffness results for HLU and spaceflight are shown in c and d respectively.

Discussion

The goal of this study was to investigate the effects of HLU on the structural properties of the tibia bone, and to compare these results to spaceflight bone loss in mice. The results demonstrated that structural properties of bone provide additional information to bone volume measurements. Spaceflight and HLU both reduced bone volume by 17%. However, spaceflight caused a greater decrease in stiffness (-34%) compared to HLU (-22%). Bone volume was expected to reduce by the same amount from both HLU and spaceflight, because studies have reported similar bone mineral density reductions in the two models, but the difference that occurred in stiffness has not been reported (Morey-Holton & Globus, 2002).

To investigate the differences between HLU and spaceflight between bone volume and stiffness further, the FE models were separated into cortical and trabecular compartments. Cortical bone reflected similar reductions in bone volume and stiffness (-14%, -32%) compared to whole bone (-17%, -34%) from spaceflight. In contrast, HLU caused a smaller reduction in bone volume (-10%) and stiffness (-15%) compared to whole bone volume (-17%) and stiffness (-22%).

Trabecular bone experienced greater relative reductions in bone volume and strength for HLU and spaceflight compared to the cortical compartments. Contrary to cortical and whole bone volume and stiffness, the trabecular bone compartment experienced greater reduction from HLU (-58%, -56%) compared to spaceflight (-32%, -45%). These results indicate that there are differences between the models that affects cortical and trabecular bone differently. The spaceflight model causes greater reductions in cortical bone stiffness, but smaller reductions in trabecular bone stiffness compared to HLU. Possible reasons for this difference may be the fluid shift in the HLU model that might affect trabecular bone more than cortical bone. Another explanation might be the difference in forces on the proximal tibia in the HLU model compared to spaceflight. The tibia bone hangs from the femur in the HLU model, and gravity is still present so there is a tensile load on the tibia cortical bone that might cause less bone resportion to occur compared to the spaceflight mice in a complete microgravity environment.

The differences that occurred in bone volume and stiffness between spaceflight and HLU can be deduced from the structural efficiency results in which spaceflight reduced structural efficiency more (-22%) than HLU (-5%). Spaceflight caused a greater reduction in stiffness compared to bone volume for whole bone, as well as cortical and trabecular bone compartments. Alternatively, HLU caused a greater reduction in stiffness compared to bone volume for whole bone and cortical bone compartments, but not for trabecular bone compartment. The greater increase in stiffness (-56%) compared to bone volume (-58%) for trabecular bone due to HLU, and the smaller reductions that occurred in cortical bone compartments in both bone volume (-10%) and stiffness (-15%) compared to spaceflight which had greater differences in reduction between bone volume (-14%) and stiffness (-32%) caused the large differences in structural efficiency between HLU and spaceflight. The greater decrease in structural efficiency in spaceflight might be caused by partial loading present in the HLU model.

Furthermore, structural efficiency results showed an increase in trabecular structural efficiency from HLU, because stiffness decreased less than bone volume. Bone remodeling occurs throughout life to maintain efficiency in the skeletal system; however, the balance between osteoclast activity and osteoblast activity is often disrupted, causing osteoporosis later in life. In these cases, it might be useful to know the efficiency of the bone structure itself: Is

more bone volume lost compared to stiffness or is the stiffness decreasing at a higher rate than bone volume? These answers could help assess bone health and fracture risk. For example, in the trabecular compartment, HLU was able to maintain stiffness more than volume (8% increase in structural efficiency), indicating that bone was lost in areas of decreased load concentration. On the other hand, spaceflight caused large decreases in structural efficiency, indicating that areas of high load concentration lost more bone than in the HLU model.

Scl-Ab mitigated the loss in BV and stiffness incurred by unloading in both models. Scl-Ab increased BV more from HLU (48%) compared to spaceflight (39%), but less effectively since structural efficiency increased less from HLU (8%) compared to spaceflight (13%). However, it is important to note that the ground controls in the spaceflight experiment increased more in bone volume (42%, 60%) and stiffness from Scl-Ab compared to HLU (37%, 48%). These differences are most likely due to differences in the cage set-ups (AEM and HLU cage). With these differences in consideration, it seems that Scl-Ab was more effective in HLU compared to spaceflight for bone volume. Partial loading might have allowed Scl-Ab to produce greater effects.

Another difference between the models that could have affected the results is differences in mobility. The spaceflight mice could use their hind limbs, and were required to climb to reach food, but the HLU mice lost all mobility in limbs when suspended by the tail. Furthermore, the stressful microgravity environment and radiation effects could have altered the bone structure, enhancing the effects seen from unloading.

Conclusions

Exposure to 13-days of unloading during spaceflight and HLU resulted in a significant decrease in bone strength in the proximal tibia. Although the HLU model produced similar results to Spaceflight for bone volume, it did not accurately approximate stiffness or structural efficiency in the proximal tibia. Separating the meshes showed spaceflight to cause a greater reduction in cortical bone volume and stiffness than HLU, but a smaller decrease in trabecular bone volume and stiffness compared to HLU. Scl-Ab caused greater increases in stiffness compared to bone volume, thereby increasing structural efficiency. Furthermore, Scl-Ab increased stiffness more in HLU compared to spaceflight; however Scl-Ab increased structural efficiency more in spaceflight compared to HLU. Structural efficiency could be a new indicator of bone health, revealing how much the change in bone volume affects stiffness. Future studies could investigate biomarkers for bone remodeling.

Acknowledgements

I would like to thank Amgen Inc, BioServe Space Technologies, and the personnel at Kennedy Space Center for their support of this project. Funding provided by the National Space Biomedical Research Institute through NASA NCC9-58, Amgen Inc, UCB-Pharma, National Space Grant College and Fellowship Program and the NC Space Grant Consortium, Summer Undergraduate Research Fellowship from the OUR at UNC-CH, and the Lucas Scholar Program at UNC-CH.

References

Bone, Henry G, Chapurlat, Roland, Brandi, Maria-Luisa, Brown, Jacques P, Czerwiński, Edward, Krieg, Marc-Antoine, . . . Resch, Heinrich. (2013). The effect of three or six years of denosumab exposure in women with postmenopausal osteoporosis: results from the FREEDOM extension. *The Journal of Clinical Endocrinology & Metabolism, 98*(11), 4483-4492.

Bonewald, Lynda F. (2013). Osteocytes *Primer on the Metabolic Bone Diseases and Disorders of Mineral Metabolism* (pp. 34-41): John Wiley & Sons, Inc.

Boskey, Adele L., & Robey, Pamela Gehron. (2013). The Composition of Bone *Primer on the Metabolic Bone Diseases and Disorders of Mineral Metabolism* (pp. 49-58): John Wiley & Sons, Inc.

Boyle, William J., Simonet, W. Scott, & Lacey, David L. (2003). Osteoclast differentiation and activation. *Nature, 423*(6937), 337-342.

Brodt, Michael D, Ellis, Cara B, & Silva, Matthew J. (1999). Growing C57Bl/6 mice increase whole bone mechanical properties by increasing geometric and material properties. *Journal of Bone and Mineral Research, 14*(12), 2159-2166.

Christiansen, Blaine A. (2013). Assessment of Bone Mass and Microarchitecture in Rodents *Primer on the Metabolic Bone Diseases and Disorders of Mineral Metabolism* (pp. 59-68): John Wiley & Sons, Inc.

de Gorter, David J. J., & ten Dijke, Peter. (2013). Signal Transduction Cascades Controlling Osteoblast Differentiation *Primer on the Metabolic Bone Diseases and Disorders of Mineral Metabolism* (pp. 15-24): John Wiley & Sons, Inc.

Ding, Ming, & Hvid, I. (2000). Quantification of age-related changes in the structure model type and trabecular thickness of human tibial cancellous bone. *Bone, 26*(3), 291-295.

Franz-Odendaal, Tamara A, Hall, Brian K, & Witten, P Eckhard. (2006). Buried alive: how osteoblasts become osteocytes. *Developmental Dynamics, 235*(1), 176-190.

Halloran, Bernard P, Ferguson, Virginia L, Simske, Steven J, Burghardt, Andrew, Venton, Laura L, & Majumdar, Sharmila. (2002). Changes in bone structure and mass with advancing age in the male C57BL/6J mouse. *Journal of Bone and Mineral Research, 17*(6), 1044-1050.

Jilka, Robert L. (2013). The relevance of mouse models for investigating age-related bone loss in humans. *The Journals of Gerontology Series A: Biological Sciences and Medical Sciences, 68*(10), 1209-1217.

Keyak, JH. (2001). Improved prediction of proximal femoral fracture load using nonlinear finite element models. *Medical engineering & physics, 23*(3), 165-173.

Keyak, JH, Sigurdsson, S, Karlsdottir, GS, Oskarsdottir, D, Sigmarsdottir, A, Kornak, J, . . . Siggeirsdottir, K. (2013). Effect of finite element model loading condition on fracture risk assessment in men and women: the AGES-Reykjavik study. *Bone, 57*(1), 18-29.

Lang, Thomas F, Leblanc, Adrian D, Evans, Harlan J, & Lu, Ying. (2006). Adaptation of the proximal femur to skeletal reloading after long-duration spaceflight. *Journal of Bone and Mineral Research, 21*(8), 1224-1230.

Lang, Thomas, LeBlanc, Adrian, Evans, Harlan, Lu, Ying, Genant, Harry, & Yu, Alice. (2004). Cortical and trabecular bone mineral loss from the spine and hip in long-duration spaceflight. *Journal of bone and mineral research, 19*(6), 1006-1012.

LeBlanc, A, Schneider, V, Shackelford, L, West, S, Oganov, V, Bakulin, A, & Veronin, L. (1996). *Bone mineral and lean tissue loss after long duration spaceflight.* Paper presented at the Journal of Bone and Mineral Research.

Morey-Holton, Emily R, & Globus, Ruth K. (2002). Hindlimb unloading rodent model: technical aspects. *Journal of Applied Physiology, 92*(4), 1367-1377.

Niebur, Glen L, Feldstein, Michael J, Yuen, Jonathan C, Chen, Tony J, & Keaveny, Tony M. (2000). High-resolution finite element models with tissue strength asymmetry accurately predict failure of trabecular bone. *Journal of biomechanics, 33*(12), 1575-1583.

Pistoia, W, Van Rietbergen, B, Lochmüller, E-M, Lill, CA, Eckstein, F, & Rüegsegger, P. (2004). Image-Based Micro-Finite-Element Modeling for Improved Distal Radius Strength Diagnosis: Moving From "Bench" to "Bedside". *Journal of Clinical Densitometry, 7*(2), 153-160.

Pistoia, Walter, Van Rietbergen, B, Lochmüller, E-M, Lill, CA, Eckstein, Felix, & Rüegsegger, Peter. (2002). Estimation of distal radius failure load with micro-finite element analysis models based on three-dimensional peripheral quantitative computed tomography images. *Bone, 30*(6), 842-848.

Ross, F. Patrick. (2013). Osteoclast Biology and Bone Resorption *Primer on the Metabolic Bone Diseases and Disorders of Mineral Metabolism* (pp. 25-33): John Wiley & Sons, Inc.

Sexson, Stephen B, & Lehner, James T. (1987). Factors affecting hip fracture mortality. *Journal of orthopaedic trauma, 1*(4), 298-305.

Somerville, JM, Aspden, RM, Armour, KE, Armour, KJ, & Reid, DM. (2004). Growth of C57BL/6 mice and the material and mechanical properties of cortical bone from the tibia. *Calcified tissue international, 74*(5), 469-475.

Spector, Elisabeth R, Smith, Scott M, & Sibonga, Jean D. (2009). Skeletal effects of long-duration head-down bed rest. *Aviation, space, and environmental medicine, 80*(Supplement 1), A23-A28.

Wigley, Cecilia. (2012). Animal Enclosure Module. Retrieved Dec. 12, 2014, from http://www.nasa.gov/mission_pages/station/research/experiments/AEM_prt.html#description

Yavropoulou, Maria P, Xygonakis, Christos, Lolou, Maria, Karadimou, Fotini, & Yovos, John G. (2014). The sclerostin story: From human genetics to the development of novel anabolic treatment for osteoporosis. *HORMONES, 13*(4), 476-487.

Appendix

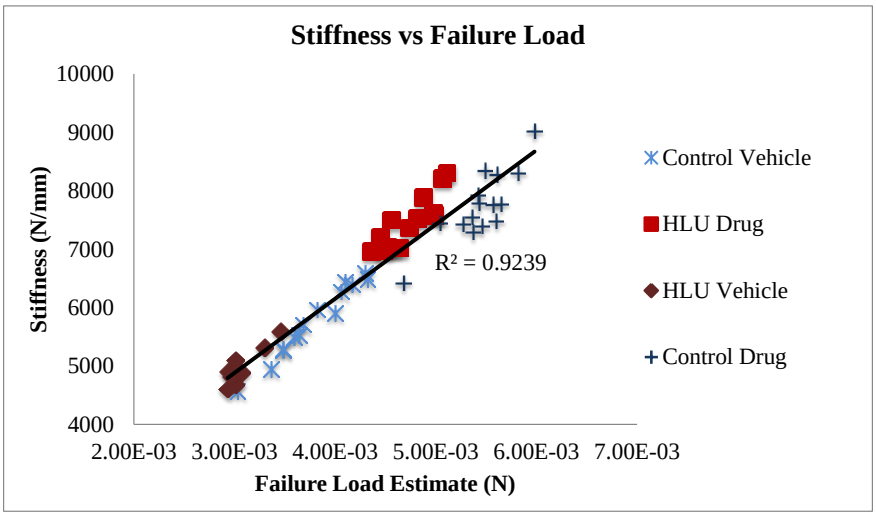

Figure 7: The correlation coefficient shown above (R^2=0.9239) demonstrates the relationship between failure load estimate and stiffness.